

Cyclisation of Citronellal to Isopulegol Catalysed by Hydrous Zirconia and Other Solid Acids

G. K. Chuah,¹ S. H. Liu, S. Jaenicke, and L. J. Harrison

Department of Chemistry, National University of Singapore, Kent Ridge, Singapore 119260

Received November 21, 2000; revised February 26, 2001; accepted February 27, 2001; published online May 15, 2001

The cyclisation of citronellal to isopulegol is an important step in the synthesis of menthol. Several zirconia-based catalysts were evaluated for this reaction. Zirconium hydroxides and phosphated zirconia had very good activity and selectivity. Ammonia TPD and pyridine IR studies indicate the presence of strong Lewis together with weak Brønsted acid sites. Other strong acids like sulfated zirconia, Amberlyst, and Nafion were very active but the selectivity toward isopulegol was poor. They catalysed side reactions such as dehydration, cracking, and etherification of isopulegol. Silica, with only weak Lewis acidity, showed very low activity. The presence of both Lewis and Brønsted sites is therefore essential for the reaction. A reaction mechanism is proposed where the citronellal molecule binds to a zirconium Lewis acid site via the aldehyde oxygen and the π -electrons of the double bond so that the right configuration is attained for cyclisation. Subsequent protonation of the aldehyde via a neighbouring Brønsted acid site initiates the cyclisation to isopulegol. © 2001 Academic Press

Key Words: citronellal; cyclisation; isopulegol; dual acid sites—Lewis and Brønsted; zirconium hydroxide; phosphated zirconia.

INTRODUCTION

The terpene alcohol, isopulegol, $C_{10}H_{18}O$, is used in the manufacture of fragrances with blossom compositions (1). Isopulegol is formed by cyclisation of citronellal. As citronellal has two prochiral carbons that become asymmetric centres in the product, four different stereoisomers are formed (Scheme 1). Isopulegol is important as an intermediate in the manufacture of menthols ($C_{10}H_{20}O$), which have a characteristic peppermint smell. Of the eight optically active menthols, only (–)-menthol, derived from the hydrogenation of (–)-isopulegol, possesses the characteristic peppermint odour and also exerts a cooling effect. The other isomers do not possess this refreshing quality.

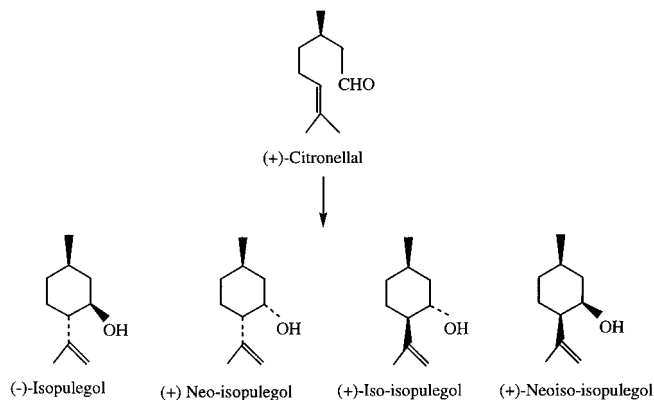
Both homogeneous and heterogeneous catalysts have been found to be active for the cyclisation reaction. Among the homogeneous catalysts, tris(triphenylphosphine)rhodium (2) as well molybdenum and tungsten carbonyl

complexes such as $PhCH_2(Et)_3N^+[Mo(CO)_4ClBr_2]^-$, $Mo(CO)_5(OTf)_2$, $[Mo(CO)_4Br_2]_2$, $PhCH_2(Et)_3N^+[W(CO)_4ClBr_2]^-$, and $W(CO)_5(OTf)_2$ have been reported (3). In the presence of these catalysts, the cis-diastereomer, (+)-neoisopulegol, was preferentially formed. The bulky ligand group in the complexes directed the shift from (–)-isopulegol to (+)-neoisopulegol. Scandium trifluoromethanesulfonate has been reported to be an efficient catalyst for selectively cyclising citronellal to isopulegol (4). The reaction has to be conducted at a subambient temperature. At $-78^\circ C$, a yield of >95% can be obtained, whereas at room temperature, the yield was only 58% due to a consecutive reaction of the formed isopulegol with citronellal. To recover the catalyst, it was necessary to extract it into the aqueous phase. Heterogeneous Lewis acids such as $ZnCl_2$, $ZnBr_2$, $AlCl_3$, $SbCl_3$, $SnCl_4$, and $TiCl_4$ offer the ease of separation and catalyse the formation of mainly (–)-isopulegol (5). $ZnBr_2$, in particular, was found to be rather efficient with 70% yield and a high selectivity of 94% to (–)-isopulegol. Arata and Matsuura (6) found that solid acids that are not affected by hydrolysis, such as $SiO_2-Al_2O_3$, $FeSO_4$, $NiSO_4$, $Ti(SO_4)_2$, $Zr(SO_4)_2$, and Al_2O_3 , also had high selectivity (>90%) and conversion (65–91%) for the isomerization of citronellal to isopulegol. In contrast, over basic CaO, little activity was noted, pointing to the importance of Lewis acid sites. Cyclisation also occurred over SiO_2 at $25^\circ C$ with 83% yield in 2 h (7). However, with all these solid catalysts, rather high amounts of the catalyst (mole ratio of catalyst to citronellal of 0.34–42) had to be used.

The solid “superacid”, sulfated zirconia, has also been reported to catalyse the cyclisation reaction (8, 9). Although a high conversion of 96% was observed, the selectivity toward isopulegol was only 46% with the main products being ethers of isopulegol and citronellal. When the sulfated zirconia was coated with a carbon molecular sieve, the selectivity increased to ~60%. This was explained by a size-exclusion effect: the smaller pore size hinders the formation of isopulegol ethers.

Zeolites with different pore sizes, e.g., clinoptilolite, mor-denite, and faujasite, were investigated in different solvents

¹ To whom correspondence should be addressed. Fax: (65) 779 1691. E-mail: chmcgk@nus.edu.sg.



SCHEME 1. Cyclisation of (+)-citronellal to isopulegol isomers.

by Fuentes *et al.* (10) for the isomerisation of citronellal. The activity correlated with the total amount of accessible Brønsted acid sites. Zeolites with smaller channels had lower activity while bigger channels increased the selectivity to isopulegol ethers. During the gas-phase reaction of citronellal with isopropanol over ion-exchanged faujasite, cyclisation was also observed (11). The formation of isopulegol was favoured by the larger pore size in LiX and NaX (ionic diameters $<2 \text{ \AA}$) where the cages offered the necessary space for the coiling of the carbon chain for cyclisation. If the zeolites were exchanged with bulky cations, e.g., Ba^{2+} , Rb^+ , and Cs^+ (ionic diameters of 2.7 to 3.4 \AA), the effective pore size was smaller and these materials catalysed preferentially the competing Meerwein–Ponndorf–Verley (MPV) reduction of citronellal to citronellol. More recently, zirconium-exchanged montmorillonite was found to catalyse the cyclisation reaction with a stereoselectivity of 90% toward (–)-isopulegol with a small amount of neo-isopulegol after 24 h in acetonitrile at 80°C (12). The yield was 91%.

This review of the recent literature indicates that acidic sites are needed for the cyclisation and that zirconium seems to have special catalytic properties. The nature of the acidic sites remains unclear as the activity has been correlated to either Brønsted or Lewis acidity. We decided to explore the use of various zirconia catalysts for the cyclisation reaction as zirconia is known to have predominantly Lewis acid sites with some weak Brønsted acidity developing after calcination above 200°C (13). As zirconium hydroxide has more hydroxyl groups than zirconia, a comparison of these two materials may be interesting. Furthermore, we have found that digesting the freshly precipitated zirconium hydroxides in the mother liquor influences the pore size and acidity of the samples (14–16). The acidity can also be modified by phosphating or sulfating the zirconia. In this study, a comparison was made with the commercially available sulfonated resin catalysts, Amberlyst 15 and Nafion SAC 13. In addition, beta zeolite and montmorillonite K10 were also

used as catalysts to study the effect of micropores and pore structure on the cyclisation reaction.

EXPERIMENTAL

Preparation and Characterization

Hydrous zirconia was prepared by precipitating a 10% zirconium chloride solution with 5 M ammonia (ca. 50% excess) (16). A part of the precipitate was removed and washed with ammonium nitrate until free of chloride, followed by a final rinse with deionized water and drying at 100°C. The remainder was subjected to open reflux at 100°C for 4 and 16 days. After the respective time, the sample was filtered off, washed, dried, and calcined at 300 or 500°C for 12 h. These samples were labelled as ZrO_2 -*D-T* where *D* stands for the number of days of digestion and *T* the temperature of calcination.

Phosphated zirconia was prepared according to Ref. (17). Hydrous zirconia digested for 4 and 16 days was washed free of chloride and dried at 100°C. It was then suspended in an aqueous solution of $(\text{NH}_4)_2\text{HPO}_4$ (8 wt%) for 1 h with constant stirring, followed by evaporation of the water and calcination at 500°C. One batch of the 500°C-calcined zirconia formed without any digestion was similarly phosphated (ZrO_2 -0-500- PO_4). Sulfated zirconia was prepared by treating the dried hydrous zirconia in 0.25 N H_2SO_4 for 1 h at room temperature using 5 cm^3 of solution per gram of solid. The resulting solid was filtered and dried at 100°C. It was subsequently calcined at 600°C for 12 h. The phosphorus and sulfur content were determined by ICP-AES and XRF. Betazeolite was prepared as described in the literature (18). After calcination at 550°C to remove the template, the zeolite was ion-exchanged with three portions of 1 M NH_4NO_3 at 80°C before calcination at 500°C to give the H-form. Silica gel 60 (Merck), Amberlyst 15 (Fluka), Nafion SAC-13 (Aldrich), Montmorillonite K10 (Fluka), and Clayzic (zinc chloride on montmorillonite K10, Fluka) were used as received.

The surface area, pore size distribution, and pore volume were determined by nitrogen adsorption using a Quantachrome NOVA 2000. The crystalline phase of the samples was determined by powder X-ray diffraction using a Siemens D5005 diffractometer (Cu anode operated at 40 kV and 40 mA). Temperature-programmed desorption of ammonia was used to determine the acidity of the samples. Typically, 0.2 g of sample was placed in a quartz reactor and pretreated in helium to 600°C for 2 h before cooling down to room temperature. Ammonia was introduced at room temperature for 15 min and the sample was flushed with helium for another 2 h before the TPD measurement. A heating ramp of 20°C min^{-1} was used to desorb the ammonia. The evolved gases were analysed using a quadrupole mass spectrometer (Hiden HAL 201) coupled to the reactor by a differentially pumped interface.

The nature of the acidic sites was probed by infrared spectroscopy of pyridine adsorbed on the samples (19). Self-supported sample wafers were mounted in an evacuable Pyrex IR cell with NaCl windows. A Bruker Equinox 55 spectrometer was used with a resolution of 2 cm^{-1} . The sample was first degassed at 300°C under vacuum for 2 h before cooling down to room temperature and being exposed to pyridine at 22 mbar. Excess pyridine was pumped off and the sample was outgassed at a vacuum of 10^{-3} mbar for 30 min before the infrared measurement. The sample was then heated to 100°C under vacuum for another 30 min and cooled to room temperature before another IR spectrum was measured. Another measurement was carried out at 200°C .

Catalytic Cyclisation of Citronellal

Racemic citronellal (Sigma) was used as received. It contained $\sim 87\%$ (\pm)-citronellal together with $\sim 13\%$ isopulegol. The reaction mixture containing 2.0 g (13 mmol) of citronellal, 15 ml of toluene, and 1 ml of nitrobenzene (internal standard) was placed in a round-bottomed flask equipped with a septum port, reflux condenser, and a guard tube. To this mixture, 100 mg of freshly dried catalyst (150°C , overnight) was added. The cyclisation reaction was carried out at 110°C in air with stirring. Samples were removed at different reaction times and the products were analyzed by gas chromatography (HP-Innowax PEG capillary column, 0.25 mm, 30 m). The conversion of citronellal was corrected for the isopulegol originally present. The different isomers were identified by GC-MS (Shimadzu) and ^1H NMR using a Bruker AMX500 (500 MHz) spectrometer. For comparison, R-(+)-citronellal (Aldrich) was also cyclised over the zirconia catalysts. The use of a chiral NMR shift reagent, europium tris {3-(hepta-fluoropropylhydroxymethylene)-(+)-camphorate} proved that the stereochemistry at the carbon-3 position was not affected by the reaction.

RESULTS AND DISCUSSION

Textural and Acidity Properties

Zirconium hydroxides dried at 300°C have surface areas of 186 to $285\text{ m}^2/\text{g}$ (Table 1). The surface area and porosity of the digested hydroxides were higher than that of undigested zirconia. The increased porosity has been attributed to the formation of a porous network due to increased oxolation between the hydroxyl groups of the zirconium hydroxide (14–16). Dehydration of the hydroxides at 500°C resulted in the formation of zirconia. $\text{ZrO}_2\text{-0-500}$ has a very low surface area of $44.1\text{ m}^2/\text{g}$ as compared to 198 and $265\text{ m}^2/\text{g}$ for the 4- and 16-days digested zirconia. The high surface area of the digested zirconia can be attributed to two effects. During digestion of the hydroxides at pH 9, some silica dissolved from the glassware and was incorporated into the samples. The zirconia formed after 4-days digestion contained 0.4%

TABLE 1
Textural Properties of Catalysts

Catalyst	Surface area (m^2/g)	Pore volume (ml/g)	Crystal phase (% tetragonal)
$\text{ZrO}_2\text{-0-300}$	186	0.15	Amorphous
$\text{ZrO}_2\text{-4-300}$	285	0.76	Amorphous
$\text{ZrO}_2\text{-16-300}$	273	0.72	Amorphous
$\text{ZrO}_2\text{-0-500}$	44.1	0.13	23.3
$\text{ZrO}_2\text{-4-500}$	198	0.49	100
$\text{ZrO}_2\text{-16-500}$	265	0.71	Amorphous
$\text{ZrO}_2\text{-0-500-PO}_4$	31.0	0.08	22.9
$\text{ZrO}_2\text{-4-PO}_4\text{-500}$	240	0.46	Amorphous
$\text{ZrO}_2\text{-16-PO}_4\text{-500}$	220	0.54	Amorphous
$\text{ZrO}_2\text{-0-SO}_4\text{-500}$	90.0	0.10	100
H-Beta zeolite	226	0.15	Si/Al 13.1
Montmorillonite K10	209	0.32	
Clayzic	149	0.21	
Silica gel 60	328	0.73	

silica by weight while the 16-days sample had 3.5% silica (analysed by x-ray fluorescence). The silica deposited in this way has an effect in stabilising the surface area of the resulting zirconia. In addition, digestion of the hydroxides leads to the removal of surface defect sites, which are responsible for grain growth during calcination. This leads to better retention of the surface area in the resulting zirconia.

All the zirconium hydroxides were x-ray amorphous, even after being heated to 300°C , but after calcination to 500°C , most of the resulting zirconias were crystalline. Zirconia formed from the freshly precipitated hydroxide, $\text{ZrO}_2\text{-0-500}$, was a mixture of monoclinic and tetragonal phases (77% : 23%). The average crystallite size was 110 Å. Zirconia resulting from hydroxides digested for 4 and 16 days were 100% tetragonal and amorphous, respectively. The crystallite size in $\text{ZrO}_2\text{-4-500}$ was ~ 48 Å, smaller than that of the undigested zirconia.

From nitrogen adsorption isotherms, the pore size distribution was calculated using the method of Barrett, Joyner, and Halenda. In $\text{ZrO}_2\text{-0-300}$, the pore size extended from micropores up to 50 Å (Fig. 1a). After calcination to form zirconia, the smaller pores collapsed, leaving pores in the range of 40 to 150 Å with an average pore size around 90 Å. The pore volume was slightly reduced from 0.15 to $0.13\text{ ml}/\text{g}$ after the formation of zirconia. The digested hydroxides, $\text{ZrO}_2\text{-4D-300}$ and $\text{ZrO}_2\text{-16D-300}$, were better able to retain their pore structure, even after calcination to 500°C (Fig. 1b). Micropores were still present in these samples.

Phosphating the zirconium hydroxide prior to calcination led to the retention of the high surface area of the hydroxide. Both the 4 and 16-days phosphated zirconia, $\text{ZrO}_2\text{-4-PO}_4\text{-500}$ and $\text{ZrO}_2\text{-16-PO}_4\text{-500}$, had surface areas over $200\text{ m}^2/\text{g}$ and pore volumes of 0.46 and $0.54\text{ ml}/\text{g}$ respectively. In contrast, $\text{ZrO}_2\text{-0-500-PO}_4$, phosphated after

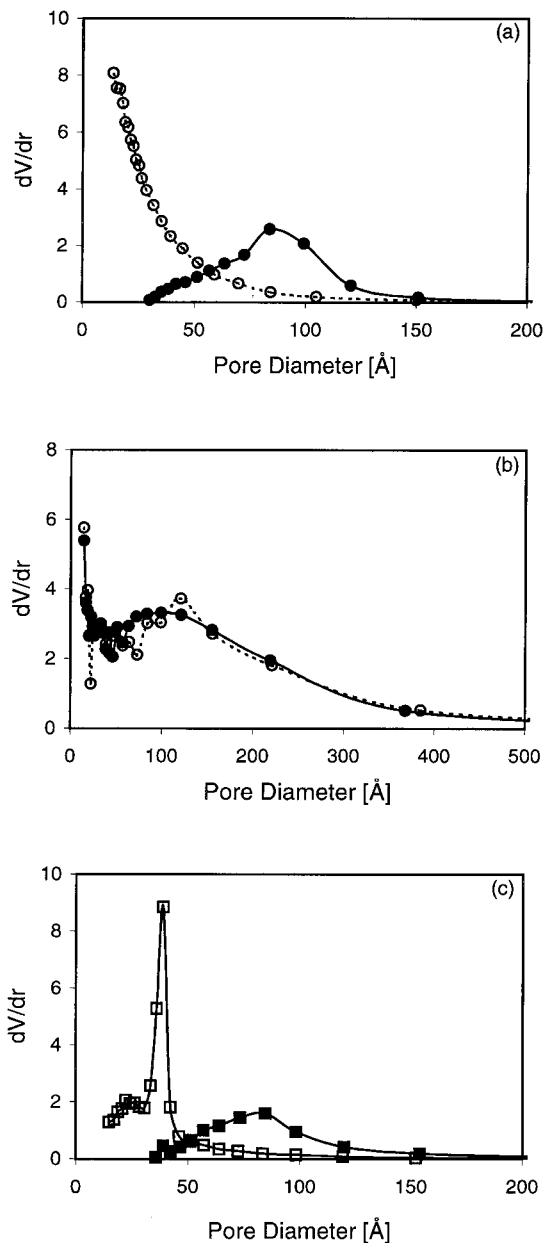


FIG. 1. Pore size distribution of (a) $\text{ZrO}_2\text{-0-300}$ (\circ), $\text{ZrO}_2\text{-0-500}$ (\bullet); (b) $\text{ZrO}_2\text{-16-300}$ (\circ), $\text{ZrO}_2\text{-16-500}$ (\bullet); (c) sulphated zirconia, $\text{ZrO}_2\text{-0-SO}_4\text{-500}$ (\square), and phosphated zirconia, $\text{ZrO}_2\text{-0-500-PO}_4$ (\blacksquare).

calcination to zirconia, had low surface area and pore volume similar to the pure support. The pore size distribution was also unchanged from $\text{ZrO}_2\text{-0-500}$ (Fig. 1c), showing that the presence of phosphate did not lead to occlusion of the pores.

Sulfated zirconia was formed from the undigested zirconium hydroxide followed by calcination, $\text{ZrO}_2\text{-0-SO}_4\text{-500}$. The presence of sulfate led to a higher surface area, $90\text{ m}^2/\text{g}$, after calcination compared to the unsulfated oxide, $44.1\text{ m}^2/\text{g}$. The pore volume of 0.10 ml/g was similar to that

of $\text{ZrO}_2\text{-0-500}$. However, the pore size distribution shows that small pores were predominant in the sample after calcination rather than big pores as in $\text{ZrO}_2\text{-0-500}$ (Fig. 1c). The pores in the sulfated zirconia had an average diameter of 45 \AA .

The acidity of the samples was compared by temperature-programmed desorption (TPD) of ammonia. As the desorption of ammonia may be completed only when temperatures of 500°C are reached, i.e., higher than the pre-treatment temperature of zirconium hydroxides, no TPD measurements were carried out for these samples. Instead, the acidity of these samples was probed by pyridine IR spectroscopy (Fig. 2). Undigested zirconium hydroxide, $\text{ZrO}_2\text{-0-300}$, showed the presence of Lewis acidity. Bands in the range of $1434\text{--}1456$, $1480\text{--}1498$, and $1560\text{--}1632\text{ cm}^{-1}$ indicate the presence of both hydrogen-bonded and co-ordinately bonded pyridine (20). After digestion, an increase in acidity was observed, indicated by a slight shift of the bands to higher wavenumbers and an increase in the absorbance of the 1490-cm^{-1} band. In addition, a weak band centred at 1540 cm^{-1} , indicative of Brønsted acidity, appeared for the digested samples. The nature of the acidic sites was not affected by subsequent calcination to form the corresponding zirconia. The increased acidity of the digested samples was also reflected by the temperature-programmed desorption of ammonia (Fig. 3). Undigested zirconia shows a broad desorption profile from ~ 50 to 500°C . The desorption profiles over digested zirconia are similar, though shifted by $\sim 20\text{--}30^\circ\text{C}$ to higher temperatures. The increased acidity of the digested samples

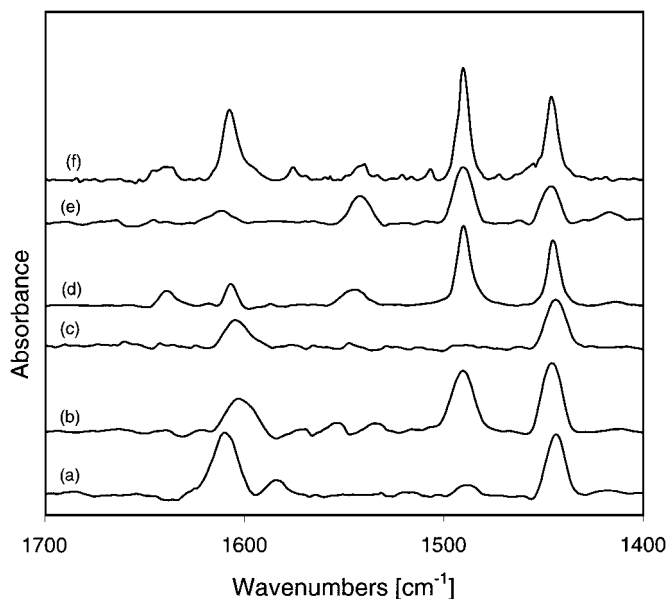


FIG. 2. Pyridine IR spectra after evacuation at 100°C of (a) $\text{ZrO}_2\text{-0-300}$, (b) $\text{ZrO}_2\text{-16-300}$, (c) $\text{ZrO}_2\text{-0-500}$, (d) $\text{ZrO}_2\text{-16-500}$, (e) $\text{ZrO}_2\text{-0-500-PO}_4$, and (f) $\text{ZrO}_2\text{-16-PO}_4\text{-500}$.

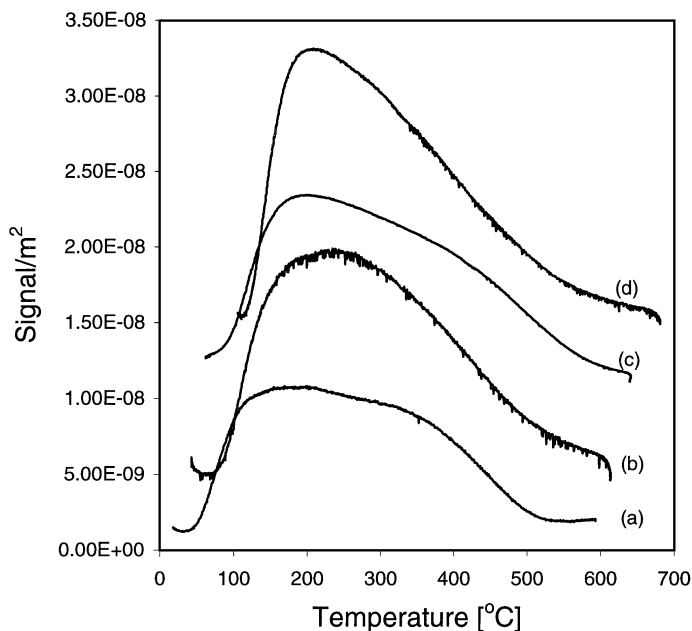


FIG. 3. Ammonia TPD profiles of zirconia and phosphated zirconia (a) $\text{ZrO}_2\text{-0-500}$, (b) $\text{ZrO}_2\text{-0-500-PO}_4$, (c) $\text{ZrO}_2\text{-4-500}$, and (d) $\text{ZrO}_2\text{-4-PO}_4\text{-500}$.

may be explained by the presence of silica. According to Tanabe *et al.* (21), acidity is generated in binary oxides due to a charge imbalance when the minor component oxide adopts the bond matrix of the major oxide. According to this model, doping of silica into zirconia gives rise to Lewis acid sites. The presence of Brønsted acidity in digested samples may be due to acidic O–H groups adjacent to the highly uncoordinated “edge” zirconium ions (19).

The ammonia desorption from phosphated zirconia, $\text{ZrO}_2\text{-0-500-PO}_4$, was narrower than the profile from unphosphated zirconia, with the main desorption occurring from 100 to 450°C (Fig. 3). Hence, both weak and strong acid sites were eliminated upon phosphating and new sites of intermediate acidity were created instead. IR spectroscopy of adsorbed pyridine shows that, in addition to the band at 1447 cm^{-1} , bands were also present at 1490 and 1540 cm^{-1} (Fig. 2). These two bands can be ascribed to Lewis and Brønsted acid sites, respectively. The pyridine IR spectra of phosphated zirconias formed by first phosphating the zirconium hydroxide, followed by calcination, also showed the presence of both Lewis and Brønsted acidity. Irrespective of whether the hydroxide or oxide was phosphated, new acidic sites of moderate strength were created, in agreement with the findings of others (22–24). Spielbauer *et al.* (17) observed that phosphate-modified zirconia had enhanced protonic acidity over that of pure zirconia. This was attributed to the presence of P–OH groups. In addition, the coordinatively unsaturated zirconium centers had increased Lewis acid strength compared to phosphate-free zirconia. The phosphate is believed to be attached to the

surface via (i) a doubly bridged mode where two of the oxygens binds to two zirconium ions and (ii) a chelate-bonding mode where two oxygens bind to one zirconium ion.

The strongly acidic nature of sulfated zirconia manifests itself in the TPD profile where the desorption of ammonia occurred from ~ 100 to 600°C (Fig. 4). In comparison, the acid strength of beta zeolite and silica is lower than that of sulfated zirconia. The peak maximum for ammonia desorption was shifted to lower temperatures in these samples. Spielbauer *et al.* (25) observed using FT-IR spectroscopy with carbon monoxide as a probe molecule that sulfated zirconia had very strong Lewis and Brønsted acidity. Pyridine IR spectroscopy showed that both Brønsted and Lewis acid sites were present in beta zeolite, K10, and Claycic while silica had only weak Lewis acidity (Fig. 5).

Catalytic Activity

Table 2 compares the conversion of citronellal and the selectivity towards isopulegol over the various samples after 1 h reaction. The mass balance was found to be within 1% for the reaction. The different diastereomers were identified by $^1\text{H NMR}$ (26). All the zirconia catalysts gave (\pm)-isopulegol as the predominant isomer, followed by (\pm)-neo-isopulegol, (\pm)-iso-isopulegol, and (\pm)-neoiso-isopulegol in the ratio of 72 : 22 : 5 : 0.4, after accounting for the isopulegol in the starting reagent, citronellal. With R-(+)-citronellal as a reactant, a similar product distribution was obtained. NMR analysis showed that (–)-isopulegol was still the main isomer, although (+)-iso-isopulegol was

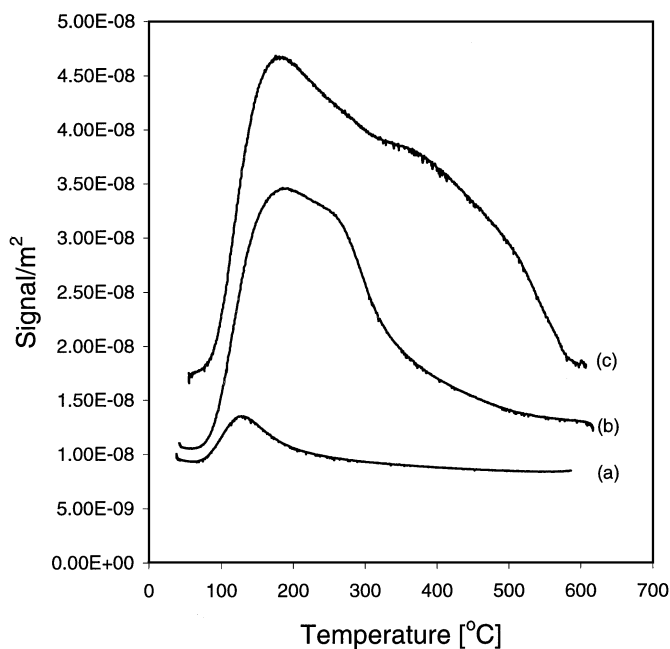


FIG. 4. Ammonia TPD profiles of (a) silica, (b) beta zeolite, and (c) sulfated zirconia.

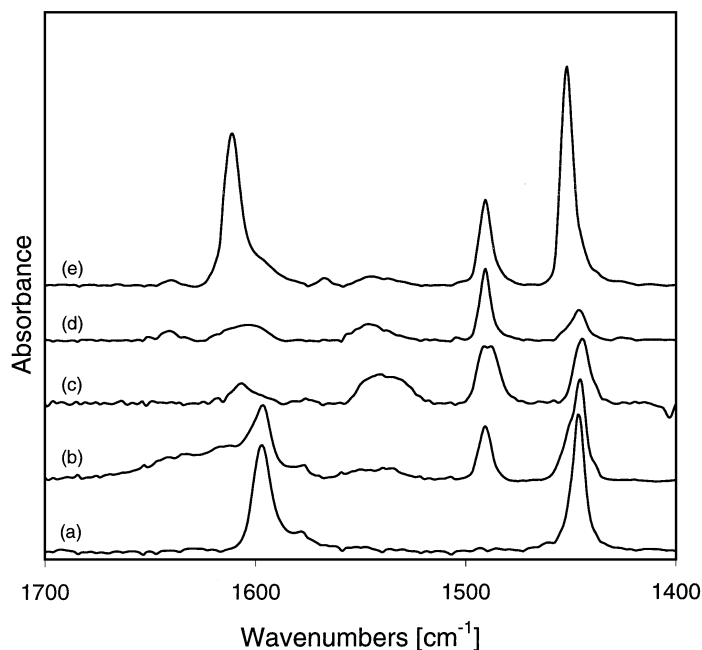


FIG. 5. Pyridine IR spectra after evacuation at 100°C of (a) silica, (b) beta zeolite, (c) sulfated zirconia, (d) K10, and (e) Clayzic.

formed in higher proportions than with the racemic reactant. The ratio of (–)-isopulegol : (+)-neo-isopulegol : (+)-iso-isopulegol : (+)-neoiso-isopulegol was 68 : 14 : 17 : 1. In addition to the isomerisation products, isopulegol ethers can be identified in some cases. These were formed by a bimolecular dehydration of isopulegol (10). Over undigested zirconium hydroxide, $ZrO_2-0-300$, the conversion was only 11% after 1 h. In contrast, the 4- and 16-days digested zirconium hydroxides were very active with 92–94% conversion of citronellal. Furthermore, the selectivity over the zirconium hydroxides was very high, 94–98%,

TABLE 2

Activity and Selectivity of Catalysts toward Isopulegol after 1 h of Reaction in Toluene

Catalyst	Conversion (%)	Selectivity (%)
$ZrO_2-0-300$	11	94
$ZrO_2-4-300$	92	97
$ZrO_2-16-300$	94	98
$ZrO_2-0-500$	0	0
$ZrO_2-4-500$	7	85
$ZrO_2-16-500$	93	99
$ZrO_2-0-500-PO_4$	97	98
ZrO_2-4-PO_4-500	95	99
$ZrO_2-16-PO_4-500$	99	99
ZrO_2-0-SO_4-500	97	52
H-Beta zeolite	95	84
K10	98	19
Clayzic	60	76
Silica gel 60	5	84

with only a small fraction of the isopulegol undergoing subsequent dimerisation to ethers. The zirconia resulting from calcining the undigested hydroxide and the 4-days digested sample were rather inactive. However, zirconia from the 16-days-digestion, $ZrO_2-16-500$, retained the high activity and selectivity of its hydroxide, with 93% of citronellal being isomerised after 1 h. This could be due to the microporous nature of the sample and/or the presence of strong Lewis combined with Brønsted acidity.

The incorporation of phosphate ions onto zirconia changes its acidic property. Indeed, after the inactive $ZrO_2-0-500$ was phosphated, the resulting material, $ZrO_2-0-500-PO_4$, was catalytically active for the cyclisation reaction (Table 2) despite its low surface area and the absence of micropores. This shows that micropores are not essential for cyclisation, but the acidity of the sample is important. On the surface of phosphated zirconia, strong Lewis acid sites coexist with some Brønsted acidity. Phosphated zirconia prepared by first phosphating the hydroxide followed by calcination was likewise highly active in the formation of isopulegol. After 1 h of reaction, the conversion in all three samples was over 95%. The used catalyst was found to contain about 0.9% by weight of organic residue as analysed by thermogravimetry.

Beta zeolite shows high activity and selectivity (84%) for the cyclisation of citronellal. By-products were due to dimerisation to isopulegol ethers, dehydration, and cracking. The ammonia TPD profile shows this sample to be less acidic than sulfated zirconia. Beta zeolite has a three-dimensional intersecting channel system where two mutually perpendicular straight channels have a cross section of 0.76×0.64 nm and the third has dimensions of 0.55×0.55 nm (27). The micropores limit any dimerisation to isopulegol ethers. NMR analysis found the isomers (±)-isopulegol : (±)-neo-isopulegol : (±)-iso-isopulegol : (±)-neoiso-isopulegol in the ratio 73 : 25 : 2 : 0.4. This is rather similar to that obtained over the zirconia catalysts, showing that the pore size has little influence on the selectivity toward the different isomers.

Sulfated zirconia is a solid superacid. It is used in this reaction to determine if strong acidity, especially Brønsted acidity, is favourable for the reaction. Although almost 100% conversion was attained within 10 min, the selectivity for isopulegol was only 61%. Several dehydration ($C_{10}H_{16}$) products of isopulegol were observed. In addition, etherification of isopulegol to various isomeric isopulegol ethers also occurred, together with further dehydration and cracking of these ethers. This results in a series of hydrocarbons with composition $C_{11}H_{22}-C_{15}H_{24}$. These reactions are catalysed by strong acidic sites that are present on the sulfated zirconia. These products increased with reaction time so that the selectivity toward isopulegol decreased to 52 and 25% after 1 and 4 h, respectively. Similarly, the two sulfonic resin catalysts, Nafion SAC-13 and Amberlyst 15, gave

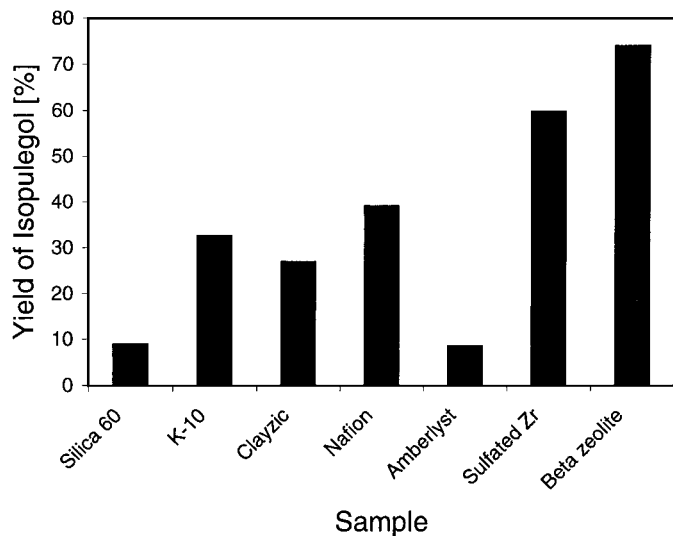


FIG. 6. Yield of isopulegol over different catalysts after 10 min of reaction except for silica (4 h).

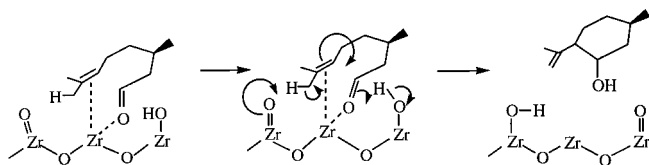
isopulegol yields of 39 and 8% after 10 min of reaction, respectively (Fig. 6).

Montmorillonite K10 was very active with 94% conversion of citronellal after only 10 min. However, the selectivity toward isopulegol was only 35% and decreased to 19% after 1 h. As with the sulfated zirconia and other strong acids, the low selectivity is due to competing reactions such as dehydration and the formation of isopulegol ethers. Our results are comparable to that of Tateiwa *et al.* (12) who obtained 41% yield of the cyclisation products in acetonitrile at 80°C after 24 h when unsupported K10 was used. Montmorillonite K10 is a layered clay consisting of octahedral aluminate modules and tetrahedral silicate SiO_4 modules in the ratio of 1 : 2 (28). The catalyst functions both as a Brønsted acid because of the coordination of a water molecule to every cation in the interlayer space and as a Lewis acid where the acid site is the aluminium atom of the clay structure. As is the case with other mesoporous supports like sulfated zirconia, the interlamellar spacing in K10 is large enough for two isopulegol molecules to undergo dimerisation to the ethers.

When ZnCl_2 was supported on the K10 support (Clayzic), a higher selectivity of 76% to isopulegol was achieved than that over K10 but the activity was lower with only 60% conversion after 1 h. When ZnCl_2 , a Lewis acid, was impregnated on clay, some of the Brønsted acid sites at the surface of the K10 support are covered, leading to better selectivity.

Silica gel showed only very low activity for the cyclisation of citronellal with only 5% conversion after 1 h. This may be due to its very low acidity deduced from the ammonia TPD profile. Furthermore, the pyridine IR studies show that only weak Lewis acid sites were present.

The cyclisation of citronellal on zeolites is believed to involve the protonation of the carbonyl group of citronellal by the acidic site, followed by intramolecular rearrangement to form a more stable carbocation and finally deprotonation to generate the isopulegol. Fuentes *et al.* (10) observed a higher reaction rate and selectivity to isopulegol with polar solvents such as chloroform. Based on these findings, they suggested that the reaction takes place through carbocations at external sites of the zeolites. Ravasio *et al.* (29) used mixed oxides such as silica–titania, silica–zirconia, and silica–alumina and observed an increase in the stereoselectivity of the cyclisation reaction when strong Lewis acid sites were present. In contrast to the findings of Fuentes *et al.* (10), no enhancement of the reaction rate was observed when using chloroform instead of toluene, hence excluding a carbocation intermediate. Although the nature of the catalytic sites was not clear, the authors suggested that the possibility of a Lewis acid catalysed mechanism is in agreement with the strong inhibition observed when dioxane was used as a solvent. In this study, we find that samples that offer strong Lewis together with weak Brønsted acidity show good activity and selectivity for cyclisation of isopulegol. Based on the catalytic and the pyridine FT-IR results, the following reaction mechanism is proposed. The coordinatively unsaturated zirconium ion acts as a strong Lewis acid site. Citronellal coordinates through the aldehyde oxygen and the electron-rich double bond onto the zirconium ion (Scheme 2). This brings the citronellal in an orientation favourable for ring closure through an intramolecular carbonyl-ene (C–C) reaction. In the transition state, protonation of the oxygen occurs via a neighbouring Brønsted hydroxyl group together with an abstraction of hydrogen from the isopropyl group followed by ring closure to form isopulegol. The surface of zirconium hydroxides, digested zirconia, and phosphated zirconia contains the active sites necessary for the cyclisation. Undigested zirconia lacks the Brønsted acid sites, while Lewis acid sites on silica are rather weak. Hence, both materials are inactive for the cyclisation reaction. The acidity of beta zeolite with a Si/Al ratio of 13 appears to be suitable for the cyclisation reaction with no side products due to strong acid-catalysed reactions like dehydration and etherification. Stronger acids such as sulfated zirconia, Amberlyst, or Nafion catalyse not only the cyclisation to isopulegol but also side reactions such as cracking and etherification.



SCHEME 2. Proposed mechanism for cyclisation of citronellal.

CONCLUSIONS

Zirconium hydroxide was found to be active and highly selective in the cyclisation of citronellal to isopulegol. Zirconia resulting from calcination of the digested hydroxides maintained the high activity of their precursors while the undigested sample was inactive. Phosphated zirconia formed by phosphating the hydroxides or oxide was also highly active for the cyclisation of citronellal. Pyridine IR studies showed that the catalytically active samples contained strong Lewis and weak Brønsted acidity. A reaction mechanism was proposed based on the coordination of the citronellal to a strong Lewis acid followed by protonation from a Brønsted acid site. Strong acids like sulfated zirconia, Amberlyst, and Nafion were also active but the yield of isopulegol was low due to side reactions such as cracking, dehydration, and etherification. Silica with very weak Lewis acidity was rather inactive. The catalytically active samples ranged from microporous beta zeolite to mesoporous zirconia.

ACKNOWLEDGMENT

Funding from the National University of Singapore (RP 000-143-051-112) is gratefully acknowledged.

REFERENCES

1. Bauer, K., Garbe, D., and Surburg, H., "Ullmann's Encyclopedia of Industrial Chemistry" (W. Gerhertz, Ed.), Vol. A11, p. 141. VCH, Weinheim, 1988.
2. Sakai, K., and Oda, O., *Tetrahedron Lett* **42**, 4375 (1972).
3. Kočovský, P., Ahmed, G., Šrogl, J., Malkov, A. V., and Steele, J., *J. Org. Chem.* **64**, 2765 (1999).
4. Aggarwal, V. K., Vennall, G. P., Davey, P. N., and Newman, C., *Tetrahedron Lett*, **39**, 1997 (1998).
5. Nakatani, Y., and Kawashima, K., *Synthesis* 147 (1978).
6. Arata, K., and Matsuura, C., *Chem. Lett.* 1797, (1989).
7. Kropp, P. J., Breton, G. W., Craig, S. L., Crawford, S. D., Durland, W. F., Jr., Jones, J. E., III, and Raleigh, J. S., *J. Org. Chem.* **60**, 4146 (1995).
8. Yadav, G. D., and Nair, J. J., *Chem. Commun.* 2369 (1998).
9. Yadav, G. D., and Nair, J. J., *Langmuir* **16**, 4072 (2000).
10. Fuentes, M., Magraner, J., De las Pozas, C., Roque-Malherbe, R., Pariente, J. P., and Corma, A., *Appl. Catal.* **47**, 367 (1989).
11. Shabtai, J., Lazar, R., and Biron, E., *J. Mol. Catal.* **27**, 35 (1984).
12. Tateiwa, J., Kimura, A., Takasuka, M., and Uemura, S., *J. Chem. Soc. Perkin Trans. 1* 2169, (1997).
13. Nakano, Y., Iizuka, T., Hattori, H., and Tanabe, K., *J. Catal.* **57**, 1 (1979).
14. Chuah, G. K., Liu, S. H., Jaenicke, S., and Li, J., *Microporous Mesoporous Mater.* **39**, 381 (2000).
15. Chuah, G. K., and Jaenicke, S., *Appl. Catal. A* **163**, 261 (1997).
16. Chuah, G. K., Jaenicke, S., and Pong, B. K., *J. Catal.* **175**, 80 (1998).
17. Spielbauer, D., Mekhermer, G. A. H., Riemer, T., Zaki, M. I., and Knözinger, H., *J. Phys. Chem. B* **101**, 4681 (1997).
18. Robson, H., *Microporous Mater.* **22**, 551 (1998).
19. Chuah, G. K., Jaenicke, S., and Xu, T. H., *Surf. Interface Anal.* **28**, 331 (1999).
20. Parry, E. P., *J. Catal.* **2**, 371 (1963).
21. Tanabe, K., Sumiyoshi, T., Shibata, K., Kiyoura, T., and Kitagawa, J., *Bull. Chem. Soc. Jpn.* **47**, 1064 (1974).
22. Busca, G., Lorenzelli, V., Galli, P., Ginestra, A. L., and Patrono, P., *J. Chem. Soc. Faraday Trans. 1* **83**, 853 (1987).
23. Boyse, R. A., and Ko, E. I., *Catal. Lett.* **38**, 225 (1996).
24. Ali, A. A. M., and Zaki, M. I., *Colloids Surf. A* **139**, 81 (1998).
25. Spielbauer, D., Mekhermer, G. A. H., Zaki, M. I., and Knözinger, H., *Catal. Lett.* **40**, 71 (1996).
26. Schulte-Elte, K. H., and Ohloff, G., *Helv. Chim. Acta* **50**, 153 (1967).
27. Jansen, J. C., Creighton, E. J., Njo, S. L., van Koningsveld, and van Bekkum, H., *Catal. Today* **38**, 205 (1997).
28. Aldridge, L. P., McLaughlin, J. R., and Pope, C. G., *J. Catal.* **30**, 409 (1973).
29. Ravasio, N., Antenori, M., Babudri, F., and Gargano, M., *Stud. Surf. Sci. Catal.* **108**, 625 (1997).